Journal of Infection and Public Health 13 (2020) 1274–1289

Contents lists available at ScienceDirect

Journal of Infection and Public Health

journal homepage: http://www.elsevier.com/locate/jiph

Review Article

Recent advancement in cancer detection using machine learning: Systematic survey of decades, comparisons and challenges

Tanzila Saba

College of Computer and Information Sciences, Prince Sultan University, Riyadh, Saudi Arabia

ARTICLE INFO

Article history:
Received 11 March 2020
Received in revised form 21 June 2020
Accepted 28 June 2020

Keywords:
Cancer
Life expectancy
Health systems
Image analysis
Machine learning

ABSTRACT

Cancer is a fatal illness often caused by genetic disorder aggregation and a variety of pathological changes. Cancerous cells are abnormal areas often growing in any part of human body that are life-threatening. Cancer also known as tumor must be quickly and correctly detected in the initial stage to identify what might be beneficial for its cure. Even though modality has different considerations, such as complicated history, improper diagnostics and treatement that are main causes of deaths. The aim of the research is to analyze, review, categorize and address the current developments of human body cancer detection using machine learning techniques for breast, brain, lung, liver, skin cancer leukemia. The study highlights how cancer diagnosis, cure process is assisted using machine learning with supervised, unsupervised and deep learning techniques. Several state of art techniques are categorized under the same cluster and results are compared on benchmark datasets from accuracy, sensitivity, specificity, false-positive metrics. Finally, challenges are also highlighted for possible future work.

Contents

E-mail address: tsaba@psu.edu.sa

https://doi.org/10.1016/j.jiph.2020.06.033

Introduction

Medical imaging analysis plays a significant role to detect abnormality in different organs of the body such as blood cancer [1–7], skin cancer [10,22–26], breast cancer [11,16,17,19], brain tumor [8,9,13–15,18,20,77], lung cancer [12,21], retina [27–29, 50] etc. The organ abnormality mostly results in tumor growth quickly which is the main death cause worldwide [30]. According to GLOBOCAN statistics, about 18.1 million new cancer cases emerged in 2018 that caused 9.6 million cancer deaths [31]. The report shows, lung cancer is foremost cause of expiry (18.4%) followed by breast cancer (6.6%), colon cancer (5.8%) prostate cancer (3.8%) and skin cancer including melanoma and non-melanoma (1.3%). It is also highlighted in the report that over one-half of the cancer demises are happened in Asia, whereas 20.3% of cancer deaths cases are reported in Europe. Different modalities such as MRI [32], PET [33], mammography [34] and CT [35] are generally used to evaluate the abnormalities in human organs [36–42,134,135].

The brain is the most complicated organ of the human body. The behavior of morphological cells in the human brain is affected by an inappropriate mitosis mechanism. During this procedure, cancerous cells are created having several morphological characteristics i.e. size and intensity. Two major brain tumor grades exist i.e. low grade and high grade. The tumor having low grade are slowly growing while the high grade is more aggressive and disturbs blood-brain supply. Therefore, most of the malignant brain tumors are called neuroepithelial tumors. Glioblastoma is frequent type of brain tumors, the ratio of this kind of tumor is 5% and the survival rate of patients is less than 5 years [43]. Most of the cancerous cells having low contrast as they compared to neighboring cells. Hence, accurate brain tumor detection is a significant task. For brain tumor detection mostly used MRI modality, a painless procedure which offers help in the analysis of tumor from several perspectives and views. Hence, the analysis of MR images is the best method to detect brain tumors among all others [44].

The existence of a nodule in the lungs could be a sign of cancer. Lung cancer is a deadly disease that needs early diagnosis to protect the life of patients. An object having round-shaped is a nodule that could be benign or malignant [45]. The malignant nodule is rapidly grown and the rapid growth of malignant nodules could affect the other organs as well. For this purpose, it is significant to treat malignant nodules at the initial stage. CT scan is the most widely employed diagnostic procedure for lung cancer. After a CT scan, more investigations are essential to detect irregular areas within the lung [12,46,47].

Breast cancer is counted as the dominant source of mortality among women. Major victims of this cancer are observed above the age of 50 years. According to ACS (American Cancer Society), about 40,610 ladies expired due to breast cancer during the year 2017 in the USA [48].

In the breast, two types of irregular cells may exist benign and malignant. Malignant cells are cancer cells and are more dangerous if repeated or meta-situated in other bodies. The benign cells are well established in type and large, whereas malignant cells are very small in number. Because of the limited size and prevalence of fatty and thick tissue, malignant tumors are very difficult to diagnose at the start of the cycle. Advanced automatic or computerized systems also need breast tumor end match identification.

Skin cancer appears as one of the rapidly prevailing diseases all over the world. Skin cancer is an uncontrolled growth of abnormal cells in the skin [22–25,49,51,136]. Skin cancer emerges in two types, melanoma, & non-melanoma. Melanoma is more dangerous than non-melanoma which is a serious kind of cancer or tumor that begins on the skin and looks like a dark spot. Sometimes, they progress from a mole to growth in size, irregular edges, itchiness, skin breakdown and color difference. In 2018, 9320 mortalities occurred due to skin cancer among 3330 females and 5990 males [52]. The ratio of Melanomas in North America, Europe, Australia and New Zealand has the highest rate and less ratio in Asia, Latin America and Africa. According to the study, if skin cancer is identified early the death ratio will be decreased by up to 90%. So cancer detection at an early stage is significant and it could provide help in decreasing the associated risk factor [10].

The type of cancer attributable to immature lymphocytes in the bone marrow is acute lymphocytic leukemia or Acute Lymphocytic Leukemia (ALL) [1,53]. Leukemia cells grow quickly and migrate to different parts of the body such as the spleen, kidneys, lymph nodes, brain and nervous system. ALL influences much of the blood and bone marrow [54]. Active childhood leukemia is most prevalent in children although recurrent and myeloid leukemia is rare in infants. Specific molecular methods have been extended to the malignancy of leukemic cell development and progeny. This hematogenic cell rise is recognized as leukemia. Acute leukemia produces blasts in the bone marrow to over 20%. It will develop rapidly and take life in a couple of months if it is not treated and managed in time [2].

The liver is an essential part of the human body which performs basic functions for example detoxification of drugs, generation of proteins needed for blood, filters the blood from waste components. Despite this, a human body faces ailment with no early indication is highly noteworthy, especially in case of a cancer diagnosis. Liver cancer is the most serious and aggressive ailment which is generally identified as hepatic cancer. Hepatocellular Carcinoma (HCC) is the most common kind of liver cancer, which causes up to 80% of victims [55]. According to GLOBOCAN report that liver cancer is the 6th and 7th causes of demises in men and females respectively worldwide. Several risk factors of liver cancer for example smoking, obesity, cirrhosis, alcoholism or hepatitis B and C are mostly related to this disease [54,56].

Scope and objectives

Different types of cancer detection and classification using machine assistance have opened up a new research area for early detection of cancer, which has shown the ability to reduce manual system impairments. This survey presents several sections on state of art techniques, analysis and comparisons on benchmark datasets for the brain tumor, breast cancer, lung cancer, liver tumor, leukemia and skin lesion detection respectively from F-measure, sensitivity, specificity, accuracy, precision points of view. The pictorial depiction of this study is presented in Fig. 1.

Benchmark datasets

This section describes benchmark datasets employed widely for experiments, analysis and comparisons of state of art techniques for cancer detection, classification. The section further highlights their source, training sets, test sets, performance measures in connection with cancer detection, segmentation and classification.

BRATS 2015 dataset

This dataset is developed by Perelman School of the Medicine University of Pennsylvania composed of total sets 274 including 192 training cases (154 HGG and 38 LGG) and 82 testing cases (66 HGG and 16 LGG). The training images contain high grade and low-grade glioma with ground truth. The ground truth is annotated with five labels such as 1 for necrosis, 2 for edema, 3 for non-enhancing tumor, 4 for enhancing tumor and 0 for everything else [132].

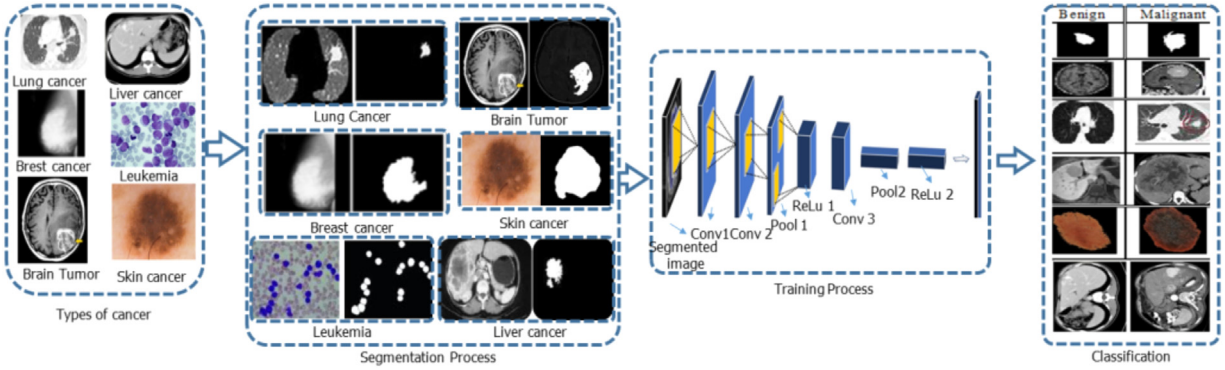

Fig. 1. Machine assisted system for cancer detection.

BRATS2016 dataset

Since the BRATS 2016 shares the same training dataset with BRATS 2015, Among 19 teams participated in the BRATS 2016. The training dataset is identical to the BRATS15 training dataset. 191 unseen datasets from both BRATS12 and BRATS13 test datasets and TCIA. Images size is 155 × 240 × 240.

Total sets 431 including 285 training cases (210 HGG and 75 LGG) and 146 testing cases for both HGG & LGG)

BRATS 2018 dataset

The datasets is updated with more routine clinically-acquired 3 T multimodal MRI scans and all the ground truth labels have been manually-revised by expert board-certified neuroradiologists.

Total sets 476 including 285 training cases (210 HGG and 75 LGG) and 191 testing cases for both HGG & LGG)

LIDC-IDRI

Lung Image Database Consortium image collection and Image Database Resource Initiative (LIDC-IDRI) is an open-source database composed of images of nodule outlines and subjective nodule characteristic ratings. The database developed to support lung nodules research and contains 244,617 images.

WBCD dataset

Wisconsin Breast Cancer Database (UCI Machine Learning Repository) holds 699 records from Fine Needle Aspirates (FNA) of human breast tissue. Each record has nine attributes. Database has a distribution of 444 (65.0%) benign samples and 239 (35.0%) malignant samples. This data set includes 201 records of one class and 85 records of another class. Each record has 9 attributes, some of which are linear and some are nominal.

FFDM dataset

Full-Field Digital Mammography hold 739 images acquired at 12-bit quantization with a pixel size of 100 × 100 μm. There are 287 biopsy-proven mass lesions, of which 148 lesions (412 images) were malignant and 139 lesions (327 images) were benign.

MIAS MiniMammographic Database (i.e. mini-MIAS database of mammograms). The database holds 322 digitized films with images of 1024 × 1024 each. Mammographic images are available via the Pilot European Image Processing Archive (PEIPA) at the University of Essex.

Digital database for screening mammography (DDSM). The Digital Database for Screening Mammography (DDSM) is one of the main source of mammographic images, produced by Massachusetts General Hospital, Sandia National Laboratories and the University of South Florida Computer Science and Engineering Department. The database composed of 2,500 sets. Every set holds two images of each breast and patient information such as age at time of scan, ACR breast density rating, subtlety rating for abnormalities, ACR keyword description of abnormalities, image information (scanner, spatial resolution). Images also hold suspicious areas, associated pixel-level ground truth information about the locations and types of suspicious regions.

ISIC Dataset: ISIC has developed a benchmark dataset of dermoscopic skin lesions images that are publically available. It explains grand challenges, problems in lesion segmentation, detection of clinical diagnostic patterns, and lesion classification, along with a high-resolution human validated training and testing set of almost 3000 CC-0 licensed images and metadata. The size of the images is not fixed due to the continuous acquisition of different kinds of visual sensors.

Atlas or DermNet: is a open source dataset holding 23,000 plus images gathered and labeled by Dermnet Skin Disease Atlas. This dataset provides a diagnosis for 23 super-classes of diseases that are taxonomically divided into 642 sub-classes.

PH2 dataset: A dataset of skin lesion named PH2 has been developed, for benchmarking and research purposes, in such a way to enable comparative study on both classification and segmentation algorithms of dermoscopic images. Which are acquired at the Dermatology Service of Hospital Pedro Hispano under similar situations through Tuebinger Mole Analyzer system using a magnification of 20 × . This is the RGB color images of 8 bit with having a resolution of 768 × 560. The dataset composed of 200 images, 80 images belong to a benign lesion, another 80 images belong to the suspicious lesion and the remaining 40 images are malignant [46,57,85].

Brain tumor

A tumor in the brain is an abnormal cell collection that has four degrees. Grade 1 and 2 brain tumors are tumors with a tendency to grow slowly and tumors with a grade 3 and 4 are cancerous (malignant) grow quicker and harder to treat [50,58–63]. There are some basic steps for tumor detection, the pre-processing phase is carried out to remove noise and non-brain tissues from input image to enhanced accuracy [65]. The brain surface extractor (BSE) techniques are employed to remove non-brain organs. The fast non-local mean (FNLM), partial differential diffusion filter (PDDF) and Wiener filter are employed to suppress noise and contrast stretching are utilized for contrast enhancement. The most popular techniques of brain tumor segmentation are Fuzzy C-means, k-means clustering and Otsu threshold methods. Similarly, U-Net architecture is also one of the famous CNN architectures employed for brain tumor segmentation. Following the process of segmentation handcrafted features are extracted to transform

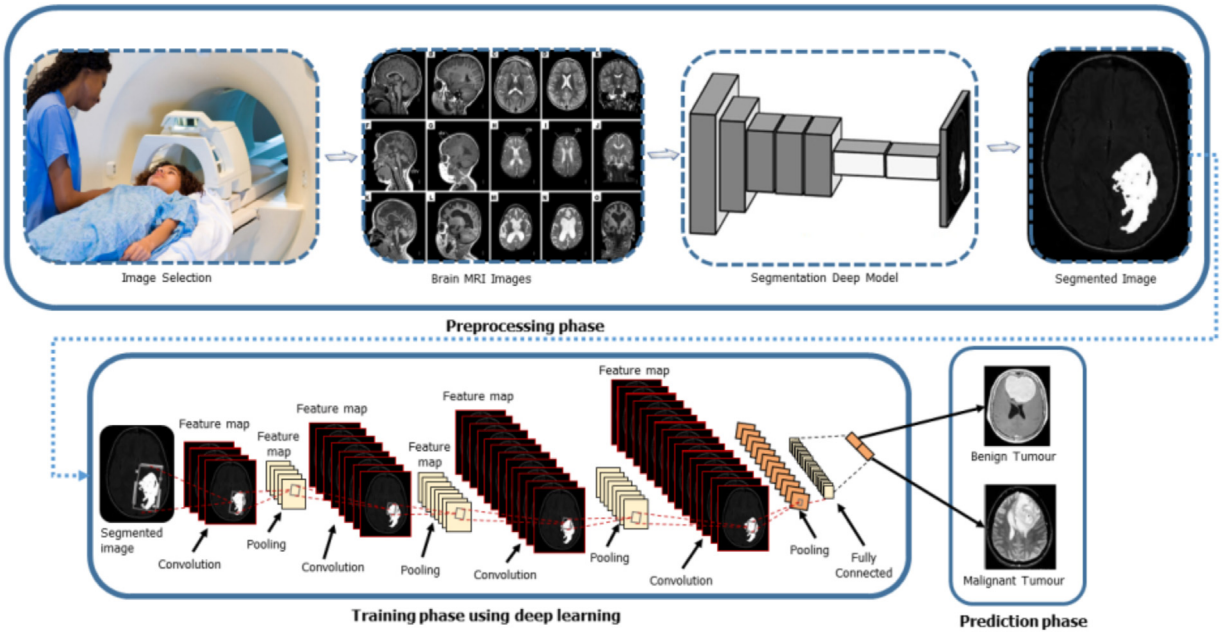

Fig. 2. Generalized framework for deep learning-based brain tumor classification.

the segmented images into mathematical descriptions. Currently, more robust techniques are employed for feature extraction, which is then used for classification. The well-known feature extraction techniques included histogram orientation gradient (HOG), Gabor wavelet transform (GWT), local binary patterns (LBP) and shape-based features. Furthermore, various feature selection and reduction techniques like a genetic algorithm (GA) and principal component analysis (PCA) are used for optimum features selection. Currently, CNN architecture is also considered a powerful technique for brain tumor detection. Fig. 2 illustrates the process of preprocessing, segmentation, training using deep learning and finally tumor prediction.

Vaishnavee and Amshakala [66] handled the problem of brain tumor segmentation utilizing SVM and self-organizing Map (SOM) strategies. Histogram equalization was done in the pre-processing stage. Four characteristics were determined to be categorized, i.e. the mean, severity, amount of incidents and variance. They used SOM clustering to identify the irregular brain clusters and segment it in the second stage. Also, brain MR photographs were categorized into different intra-tumor groups. To conduct this characterization of the gray level co-existing texture matrix (GLCMs) in sub-tumor levels, a Principle Component Analysis (PCA) used to measure these texture characteristics as a step towards reducing dimensionally. The achieved accuracy is reported in Table 1; however, the authors did not compare results in state of art and there was no justification for using SVM and SOM.

Nie et al. [68] reported a complete automatic 3D-CNN brain tumor segmentation systems utilizing both T1, MR test (MRI) and Diffusion Tensor Imaging (DTI). Different pre-processing strategies were measured using T1, DTI tensor and fMRI-specific BLD (blood oxygen-dependent) variance rate for increasing MR modality i.e. strength standardization. The extractor function was 3D-CNN and the final prediction was carried out by SVM with 89.9% (accuracy), 92.19% (sensitivity), 88.22% (specificity). However, the proposed system is computationally expensive and is unsuitable for large dataset.

Arikan et al. [76] proposed a semi-automated, collaborative seed selection-based SVM approach for the fragmentation of brain tumors. They used anisotropic diffusion filter in the MR images during the pre-processing stage to eliminate noise. Random seeds would then be chosen for the SVM classification from the previously processed MR images. For success evaluation, a freely accessible BRATS 2015 dataset was used. To test the outcomes of the new procedure they picked four patients from the MICCIA BRATS-2015 data collection. Their solution obtained an average Dice Similarity (DS) of approximately 81% relative to the basic reality. Ellwaa et al. [67] proposed a fully automatic segmentation approach for MRI-based brain tumors utilizing the iterative random tree. The accuracy of the patient with specific details in the data set used for random forest classification was enhanced iteratively. The technique tested on BRATS-2016. Selection requirements for the individual with the strongest knowledge lead to positive outcomes. However, no justification was provided about the selection requirements and no accuracy results reported. Abbasi and Tajeripour [71] proposed a 3D automated interface for brain tumor detection and segmentation on BRATS 2013 dataset. For pre-processing, bias field correction, histogram communication, ROIs (Region of Interests) and are isolated from the FLAIR image context. For learning tasks, HOG and LBP features were fed to random forest classifier. However, they used synthetic data for experiments and reported an accuracy of 93%.

Mehmood et al. [73] proposed an effective system for brain imaging and simulation using MR images. In the beginning, there is an immersive, semi-automated 3D segmentation technique that essentially separates the brain and tumor regions from the MR parts using SVM 95.53% accuracy, 99.49% sensitivity, 99.0% precision and 0.09 mean square error. However, experiments performed on self-generated datasets. Das et al. [74] detected normal and abnormal tissue samples by using texture-based features. 80 images of abnormal and normal tissue were used obtained from GMCH, Guwahati Hospitals. Five descriptors fusion (LBP, Tamura, HOG, GRLN, and GLCM) extracted features from the images and formulated 172 features vector set. Additionally, six classifiers i.e. SVM, K-NN, Logistic Regression, Quadratic Discriminant, Linear Discriminant used to evaluate the performance of each feature set both in the group and individually. The experimental results demonstrated 100% accuracy using the complete feature set as compared to individual sets of features and it enhanced the average classification accuracy to 98.6%. They concluded that the computer-aided system could lead to better diagnosis as child-hood brain lesions are very critical. The

Table 1
Current methods, dataset and result for brain tumor detection.

Reference	Methodology	Datasets	Results
Vaishnavee and Amshakala, [66]	PSVM	BRATS -2015	92 (Accuracy) 94 (Recall) 93 (Precision)
Ellwaa et al., [67]	Iterative Random Forest	BRATS-2016	
Nie et al., [68]	3D-CNN with SVM	Self Generated	89.9(Accuracy) 92.19(sensitivity) 88.22(Specificity) 84.44(PPR) 95.57(NPR)
Wasule and Sonar, [69]	SVM and K-NN	BRATS 2012	96 (Accuracy) 100 (Precision) 76 (Recall) 86.4 (F-Measure)
Fidon et al., [70]	CNN	BRATS-2013	
Abbasi and Tajeripour, [71]	RF	BRATS-2013	
Iqbal et al., [72]	CNN	BRATS 2015	82.29 (Accuracy)
Mehmood et al., [73]	Bow-Surf based SVM	LRH	99 (Accuracy) 0.96 (sensitivity) 0.99 (Specificity) 0.05 (FPR) 0.099 (FNR) 0.98 (F-Measure)
Das et al., [74]	Multiple classifiers fusion	GMCH	100 (Accuracy) 1.00 (AUC)
Saba et al., [75]	VGG-19	BRATS -2015 BRATS -2016 BRATS-2017	0.9878(Accuracy) 0.9963(Accuracy) 0.9967(Accuracy)

RF (Random Forecast), 3D-CNN (three-dimensional convolution neural network), SVM (Support Vector Machine), KNN (K Nearest Neighbor), CNN (Convolution Neural Network), BoW (bag of words), SURF (speeded up robust features), GMCH (Guwahati Medical College), GLCM (grey level co-occurrence matrix), GRLN (grey level run length matrix), LBP (local binary pattern), PSVM (Proximal Support Vector Machines), VGG (visual geometry group), LRH (Lady Reading Hospital), BRATS (Brain Tumor Segmentation), DSC (Dice Similarity Coefficient), NPR (Negative Predictive Rate), PPR (Positive Predictive Rate), AUC (Area Under the Curve).

use of several classifiers makes the system slow and computationally expensive.

Iqbal et al. [72] proposed a deep learning model for reliable brain tumor delineation from Medical Benchmarks, utilizing short-term memory (LSTM) and coevolutionary neural networks (ConvNet). The two different models ConvNet and LSTM are equipped using the same data set and create a group to maximize the performance. The two separate models are merged. A data collection consisting of MRI images in four modalities T1, T2, T1c and FLAIR is widely accessible for this reason. MICCAI BRATS 2015 is accessible. To boost image clarity, several variations are designed and optimal output variations are added to the preprocessing approaches including noise reduction, histogram equalization and edge enhancement. Class weighting is used in the current models to address the issue of class inequality. Validation details from the same image collection are checked on the learned model, and findings from each experiment are recorded. ConvNet as a single score (exactitude) of 75% while 80% is produced by an LSTM-based network, with a total fusion of 82.29%. The suggested Grab cut approach [75] is implemented to specifically segment real losses symptoms while the Visual Geometry Transfer Learning System (VGG-19) is completed to produce features that are then assembled (shape and texture) by series. Such technologies are designed by entropy to reliably and easily identify and to transmit fused vectors to classification units. The described model is tested in the MICCAI challenge databases including multi-modal brain tumor segmentation (BRATS) 2015, 2016 and 2017 respectively, utilizing top scientific image processing and computer-assisted intervention. The study findings with a coefficient of dice similarity (DSC) hit 0.99 using 2015 BRATS, 1.00 on 2016 BRATS and 0.99 using 2017 BRATS. However, they did not use other classifiers or their fusion to verify the viability of their technique.

Most recently, Ramzan et al. [78] segmented multiple brain regions using 3DCNN with residual learning and extensive convolution to effectively apprise end-to- end mapping between MRI volumes & voxel-level brain segments. Mean 0.879 and 0.914 dice scores were obtained for 3 and 9 brain regions using data from 3 different sources. In comparison, for 8 brain regions with MRBrains18 data collection, a mean dice score of 0.903 is higher than 0.876 obtained in the last study. Similiary, to detect brain abnormalities from MR Images analysis, Nayak et al. [61] proposed CNN model composed of five layers (four Convolutional layers and one fully-connected layer) with learnable parameters. To check the viability of their model two benchmark multi-class brain MRI datasets namely, MD-1 and MD-2 employed. Authors claimed 100% and 97.50% classification accuracy on MD-1 and MD-2 datasets respectively.

Lu et al. [59] proposed a deep learning CNN ResNet based on the pyramid dilated convolution for Gliomas classification. Experiments were performed on a local clinical dataset and 80.11% glioma classification accuracy attained. However, they did not use benchmark dataset for experiments. Table 1 presents a summary of existing methods for brain tumor detection, methodologies adopted, dataset and results.

Lung cancer

Lung cancer is one of the world's most popular causes of death from the lungs. A variety of operational, percutaneous and surgical treatments will benefit several patients if the condition is a tiny, diffuse tumor. Unfortunately, as there are few without any signs in the early phases of illness, a diagnosis of progressive clinical illness, nodal progression and/or metastatic disease in 75 percent of lung cancers emerge later. According to Australian research, the overall survival rate of patients diagnosed with lung cancer is 15% [88]. Several researchers have reported their work in the field of lung nodule detection and classification using LIDC/IDRI Database. The Database composed of 240000 plus images of nodule.

The usage of machine learning techniques helps in early diagnosis and evaluation of lung nodules by processing CT images

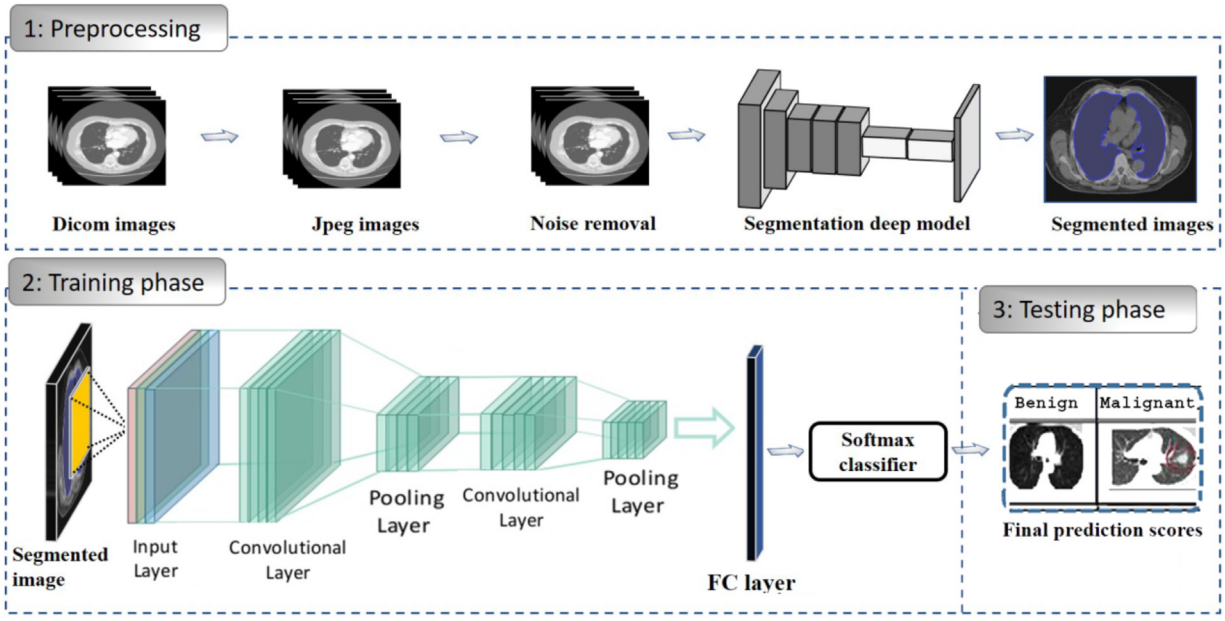

Fig. 3. Machine supported framework for lung nodules prediction.

constructed through artificial intelligence methods. Such systems are called decision support systems that investigate the images through preprocessing, segmentation, feature extraction and classification process presented in Fig. 3.

Multi-Convolution Neural Networks (MCNN) is employed to capture nodular heterogeneity through extracting discriminative features from alternately stacked layers. For the evaluation of the proposed LIDC-IDRI method, lung nodule screening and annotation are used. In this method, three CNN is used in the MCNN model, in which parallel nodule patches with varying sizes are assembled as inputs. They used LIDC- database, the segmentation method accuracy is 97 %. Setio et al. [79] proposed a method to detect Pulmonary Nodule, used a multi-view Convolution network for model training. Three algorithms fused for candidate nodule detection i.e. large-solid, sub-solid and solid for accurate detection of all suspicious nodules. The proposed system is trained and validated on publicly available LIDC-IDRI dataset. The sensitivity level achieved by the research work is 85.4% at 1 and 90.1% at 4 false-positives. respectively. Dou et al. [80] used a new technique to decrease false-positive in automated detection of the nodule by using 3-DCNNs from volumetric CT scans. This technique has been extensively validated in the challenge of LUNA16, where they achieved the highest CPM score decreasing of the false-positive track.

Shen et al. [81] introduced a new classification system for lung nodules in high suspicion and low suspicion. For this method, the multi-crop convolution neural network is used by utilizing a modern multi-crop pooling strategy to derive valuable knowledge from nodule by cutting regions from convolutional characteristics maps and by using maximal pooling times. Appreciation to this method, they obtained a good 87.14% classification precision and 0.93% CUP scoring using the LIDC-IDRI data. Van-Griethuysen et al. [82] PyRadiomics proposed the characterization of lung nodules to differentiate nodules into malignant nodules or benign nodules. They used publicly available LIDC data sets cohort, an algorithm implemented in Python, to provide a front end code that could be used for the 3D slicer. Tahoces et al. [83] suggested a methodology utilizing a simple incremental approach to measure 3D aortic lumen geometry from an initial contour within. The tests of the proposed algorithm for a mean DSC of 0.951 were always greater than 0.928 for use in the full datasets and measured 3D portions of the 16 case of CT. For the 16 cases chosen, the median distance was less than 0.9 mm. In terms of accuracy, the proposed solution is outstanding and the high-quality outcome could be obtained for rare and normal situations. However, the experimental setup employed was not clearly explained and results were not compared in the state of art.

Xie et al., [133] proposed a new automatic 2D neural Convolutional Neural Network (CNN) pulmonary nodule detection system to improve the CT reading process. First, change the configuration of Faster R-CNN to classify nodule candidates with two area proposal networks and a deconvolution layer with three models is equipped for three forms of slices for eventual outcome fusion. Second, an improved 2D CNN architecture is designed to achieve a false positive elimination, which is a classifier that separates real nodules from candidates. For the retraining phase a pattern that improves susceptibility to pulmonary nodule identification. Finally, the tests are mixed to vote on the final results of the group. Comprehensive tests are conducted in LUNA16, with a sensitivity of 86.42 %. The accuracy at 1/8 and 1/2 FPs/scan is 73.4%, and 74.4% respectively for the false-positive reduction. The proposed method demonstrated that accurate pulmonary nodule identification could be accomplished. However, the reported accuracy is not as per state of art.

Jiang et al. [84] suggested the successful identification of lung nodules based on multi- patches cut out of the Frangi filter's lung image. A four-channel neural network model designed to collect radiologists' information for the identification of nodules from four layers through the integration of two image classes. For 4.7 false-positives for each scan and a 94% sensitivity of 15.1 false-positive ones per sample, 80.06% of the sensitivity could be obtained. They concluded that the patch-based learning method in multiple groups is successful for improving the performance and false-positive lessens dramatically in a large quantity of image data. Naqi et al. [85] proposed a nodule system of identification and diagnosis, consisting of four central steps. First of all, the abstraction of the lung area is based on the optimum gray- threshold determined with the optimization of Darwinian particles. Then a new method for the identification of candidates is introduced, focused on the spatial health of the nodules, in a parametric system. A hybrid geometrical texture description built in the next step to better represent the nominee nodule, a mixture of both 2D and 3D knowledge regarding

applicants of the nodule. Ultimately, a profound thinking approach was introduced to that false-positive effects, focused on the stacked autoencoder and softmax. The Lung Image Database Collaboration and the Image Database Network Project, the biggest accessible publicly usable database, shows that the suggested solution dramatically decreased the amount of false- to 2.8 per scan with encouraging sensitivities of 95.6%. An automatic nodule identification and the sorting method suggested by Naqi et al. [86]. A modern 3D nodule hybrid sensors process, including the Active Contour Model (ACM), 3D neighborhood networking, and the rules-based on the spatial characteristics introduced in the next step. By integrating geometric texture with the Oriented Gradient Histogram (PCA) for each nodule nominee, a hybrid feature vector is generated using a Principle Component Analysis (HOG-PCA). The sorting is carried out with 4 separate classifiers, namely Naive Bayesian, Support Vector Machine (SVM), and Adaboost. After the abstraction process is finished by the introduction of four different classifications. The evaluation is carried out in a sample of the Lung Image Database Consortium (LIDC). AdaBoost has succeeded in terms of precision, responsiveness, specificity and scan all other classifiers. However, Naqi et al. [86] approach is computationally expensive and demands several resources as well as accuracy is not better than others reported in state of art.

Asuntha and Srinivasan [87] presented a modern deep learning strategy for the identification of lung nodules by using HoG, WT, LBP, SIFT and Zernike Moment for attribute extraction. Upon extraction, selection of the best feature rendered using the Fuzzy Particle Swarm Optimization (FPSO) algorithm. Dark leather is ultimately used for classifying these characteristics. CNN computational complexity is reduced by a current FPSOCNN. Table 2 presents a detailed comparison of current methods of lung cancer detection on LIDC-IDRI dataset. Saba [46] presented an automated approach for lung nodule detection and classification composed of four main stages. Preprocessing, segmentation, features extraction and candidate's lesion detection. The author employed multiple classifiers including logistic regression, multilayer perceptron, and voted perceptron for lung nodule classification using k-fold cross-validation process and attained 100% accuracy on LIDC dataset.

Skin cancer

The machine-assisted systems employing dermoscopic images have been started form the last few decades to help the dermatologists clinical decision and to detect highly suspicious cases. The intelligent systems could also be used as an extra tool by non-experienced clinicians to achieve an initial assessment and to increase the patient follow up process [91,136]. Roughly, such systems are divided into two major classes concerning meaningful feature extraction from dermoscopic images In which one class used medical procedure of diagnosis and extract automatically the same medical features i.e. symmetry, several colors, atypical differential structures. Additionally, another class is based on machine learning to recognize statistical patterns and applied to image features i.e. texture and color features [92]. In most of the work, the focus is on the development of machine learning techniques with advanced features extraction, such ABCD rule, a 3-point checklist. Therefore DCNNs accomplished major outcomes in the field of medical imaging, through which features are generated directly from the images. Fig. 4 illustrated the handcrafted and CNN feature extraction framework.

In another technique reported by Ramya et al. [93], for the pre-processing stage, the authors used an adaptive histogram equalization technique and wiener filter. In their research, they used an active contour segmentation mechanism. The features used in the system are extracted using GLCM and for the classification of the skin lesion into malignant or benign they used SVM classifier, a sensitivity of 90%, accuracy of 95% and a specificity of 85% is observed. However, they used a small dataset for experiments.

Premaladha and Ravichandran [94], proposed an intelligent system for efficient classification and predication of melanoma. Median filter and Contrast Limited Adaptive Histogram Equalization methods used for image enhancement. A novel technique for segmentation (Normalized Otsu's Segmentation) used to segment lesion from skin. Which reduced the variable illumination problem. From the segmented images, fifteen features extracted and fed into the proposed classifier (neural networks based on deep learning and hybrid AdaBoost SVM). The system tested and validated with almost 992 images belongs to benign and malignant lesions and it achieved 93 % classification accuracy.

Bareiro Paniagua et al. [57], technique input a Dermoscopy image and the diagnosed lesion is malignant or benign. This technique composed of the next modules: preprocessing of an image, segmentation of lesion, extraction of features from a lesion, and finally classification. In a pre-processing step, remove unwanted details i.e. hairs. ABCD rule used to extract features of the prior segmented affected regions. Finally, lesions classified into malignant or benign using Support Vector Machine (SVM). Experimental results illustrated that the proposal has an accuracy of 90.63 %, the sensitivity of 95 %, and specificity of 83.33 % on a dataset of 104 Dermoscopy images. These results are promising as the diagnosis performance by traditional progress in the dermatology area.

Khan et al. [21] utilized textural, and color features which are very common for image analysis. These methods mostly employed handcrafted features which degrades the efficiency of machine-assisted framework. Likewise, Aima and Sharma [95], handles early stage melanoma skin cancer detection using CNN experimented on 514 dermoscopic images of ISIC dataset. They achieved accuracy of 74.76% and validation loss of 57.56%. Dai et al. [96] proposed a CNN model and pre-trained 10,015 images of skin cancer using a smartphone where the inference process takes place. To test a new input all computations were performed locally where the test data persists. However, their method decreased latency, saves power, and increased privacy with 75.2% model accuracy. The reported accuracy is far below than reported in the literature. Saba et al., [10] proposed an automated approach for skin lesion detection and recognition using a deep convolutional neural network (DCNN) composed of three stages, contrast enhancement, lesion boundary extraction, in-depth features extraction. Discriminant features were seleted using an entropy approach.The proposed method is tested on PH2 and ISIC 2017 datasets, whereas the recognition phase is validated on PH2, ISBI 2016, and ISBI 2017 datasets. Authors claimed superiority of their approch on existing methods with an accuracy 98.4% on PH2 dataset, 95.1% on ISBI dataset and 94.8% on ISBI 2017 dataset.

For indepth review of skin cancer readers are referred to Arthur and Hossein [97] and Barata et al. [91]. Table 3 exhibits the current skin lesion procedures, results, and comparisons of benchmark datasets.

Acute Lymphoblastic Leukemia (ALL) detection

Acute lymphocytic leukemia (ALL) is a type of cancer of the blood and bone marrow. Literature reveals different machine-assisted Acute Lymphoblastic Leukemia (ALL) classification techniques in health applications [1,2].

White Blood Cells (WBC) segmentation involves separating the cell from its background, often through the identification of the cell's cytoplasm and nucleus [99]. This is readily achieved through image processing functions available in medical software. Converting the image to a different color space, contrast stretching,

Table 2
Current methods, dataset and result for lungs cancer detection.

Reference	Methodology	Dataset	Results (%)
Saba, [46]	Multiple classifiers voting	LIDC	100 (Sensitivity)
Shen et al., [88]	Multi-scale Convolutional Neural Networks (MCNN)	LIDC-IDRI	86.84 (Accuracy)
Kumar et al., [89]	deep feature with auto-encoder	LIDC	75.01 (Accuracy) 83.35 (Sensitivity) 0.39 (false positive)
Firmino et al., [90]	Watershed, HoG and SVM	LIDC-IDRI	97 (Accuracy) 94.4 (Sensitivity) 7.04 (false positive)
Setio et al., [79]	multi-view ConvNet	LIDC-IDRI	sensitivity of 85.4% and 90.1% at 1 and 4 FPs/scan
Shen et al., [81]	Multi crop convolution neural network	LIDC-IDRI	87.14 (Accuracy) 0.77 (Sensitivity) 0.93 (Specificity) 0.93 (AUC)
Jiang et al., [84]	Frangi filter with 4-channel CNN	LIDC-IDRI	sensitivity of 80.06 % and 94% at 4.7 and 15.5 FPs/scan
Naqi et al., [85]	Hybrid geometric texture feature descriptor, auto-encoder and softmax.	LIDC-IDRI	96.9 (Accuracy) 95.6 (Sensitivity) 97.0 (Specificity) 2.8 (FPs/scan)
Xie et al., 2019	2-D CNN, Faster R-CNN	LIDC-IDRI	86.42 (Accuracy) Sensitivity of 73.4% and 74.4% at 1/8 and 1/4 FPs/scan
Naqi et al., [86]	HoG, PCA, Texture and geometry feature. K-NN, Naive Bayes, SVM and AdaBoost	LIDC	99.2 (Accuracy) 98.3 (Sensitivity) 98.0 (Specificity) 3.3 (FPs/scan)
Asuntha and Srinivasan, [87]	HoG, WT, LBP, SIFT and Zernike Moment feature descriptor. FPSOCNN are used for classification	LIDC	95.62 (Accuracy) 97.93 (Sensitivity) 96.32 (specificity)
Khan et al., [21]	GLCM, LBP, Color Features using SVM classifier	DermIS	96% (Accuracy) 97% (sensitivity) 96% (specificity) 97% (precision)

MCNN (Multi-scale Convolutional Neural Networks), HOG (Histogram of oriented gradient), SVM (Support vector machine), ConvNet (Convolution neural network), CNN (Convolution neural network), 2-D CNN (two-dimensional convolution neural network), Faster R-CNN (Faster recurrent convolution neural network), PCA (Principle component analysis), K-NN (K-Nearest neighbor), FPSOCNN (Fuzzy Particle Swarm Optimization Convolution Neural Network), SIFT (Scale Invariant Feature Transform), LBP (Local Binary Pattern), LIDC (Lung Image Database Consortium), LIDC-IDRI (Lung Image Database Consortium-Image Database Resource Initiative).

Table 3
Current methods, dataset and result for skin lesion detection.

Reference	Methodology	Dataset	Results
Saba et al., [10]	Deep convolutional neural network (DCNN)	PH2, ISBI 2016, and ISBI 2017	98.4% on PH2 dataset, 95.1% on ISBI dataset and 94.8% on ISBI 2017 dataset
Ramya et al., [93]	Used active contour segmentation mechanism. GLCM feature and for the classification they used SVM classifier	ISIC	95% (Accuracy) 90% (sensitivity) 85% (specificity)
Premaladha and Ravichandran, [94]	Median filter and Contrast Limited Adaptive Histogram Equalization and Normalized Otsu's Segmentation is used. neural networks and hybrid AdaBoost SVM is used for classification	Skin Cancer and Benign Tumor Image Atlas - Contents	91.7% (Accuracy) 94.1%(sensitivity) 88.7%(specificity) 0.83%(Kappa)
Bareiro Paniagua et al., [57]	Feature are extracted using ABCD rule and the extracted feature is classified using SVM	PH^2	90.63% (Accuracy) 95% (sensitivity) 83.33%(specificity)
Li and Shen, [98]	FCRN	ISIC	0.912%(AUC) 0.857% (Accuracy) 0.490%(sensitivity) 0.961%(specificity) 0.729%(average precision)
Aima and Sharma, [95]	ANN	ISIC	74.76% (Accuracy) 57.56% (validation loss)
Dai et al., [96],	CNN	Large collection of Multi-Source Dermatoscopic Images	75.2 (Accuracy) 0.71 (validation loss)

GLCM (Gray Level Cooccurrence Matrix), SVM(Support Vector Machine), ABCD (Asymmetry, Border, Color, Diameter), FCRN (Fully Convolutional Residual Networks), LBP (Local Binary Pattern), ANN (Artificial Neural Network), CNN (Convolution Neural Network), ISIC (International Skin Imaging Collaboration), AUC (Area Under the Curve).

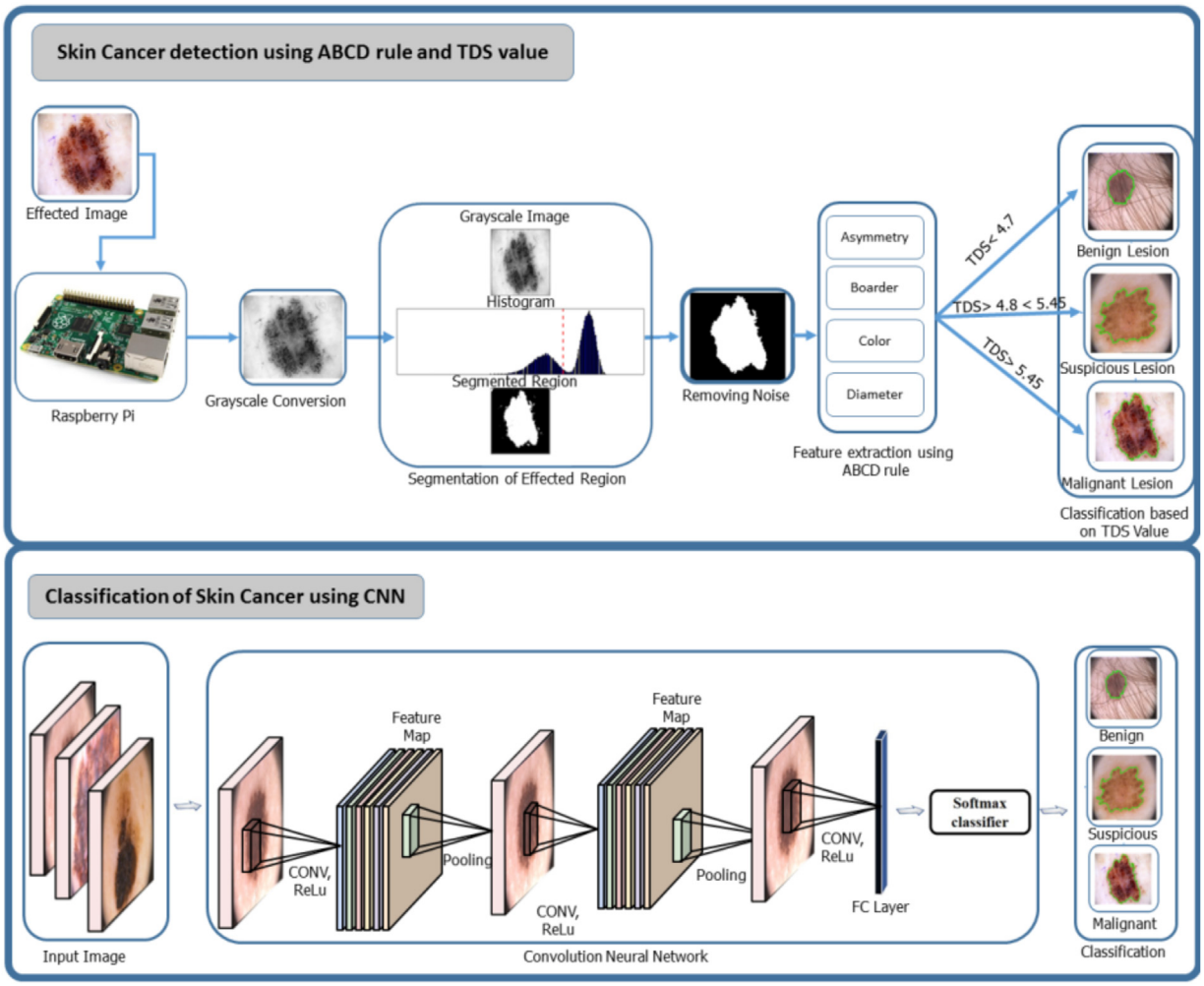

Fig. 4. Handcrafted and CNN feature extraction framework for skin cancer.

thresholding, cauterization, water-shedding, and morphological filtering are some steps mentioned in the literature [100,101]. These steps may produce a binary image of white WBC components for masking the original color image [102]. In multiple works, WBC segmentation exploited morphological observations from gray-scale microscopic images. Since WBCs stain is darker than other blood components, contrast stretching was performed to enhance their nuclei. Then a morphological filter was derived by averaging the WBC diameters. Applying this morphological filter further enhanced WBC nuclei while reducing smaller blood components. These steps produced sub-images of fixed dimension containing centrally located WBCs with high accuracy. Putzu et al. improved this strategy by inserting additional color-space conversion and thresholding steps. Also, grouped WBCs were separated through watershed segmentation yielding 92% accuracy [102]. The detection and classification of ALL are shown in Fig. 5.

Normally to detect Acute Lymphoblastic Leukemia (ALL), physicians check microscopic images manually, which is a lengthy process and reduces accuracy. Patel and Mishra [103] proposed an automated approach to determine leukemia at an early stage. They proposed some filtering methods (k-state grouping, histogram alignment, and zack) and employed SVM for classification purposes. The proposed system successfully implemented in MATLAB and an accuracy of 93.57% reached. However, they performed experiments on a small dataset.

Khalilabad and Hassanpour [104] designed the automated system to evaluate the data collected from micro-images to identify blood cancer cases. The proposed framework comprised of three major components of 'photography, data minerals, and diagnosis. The image analysis level operates such as image generalization, gridding, and extracting image data. Information Management includes information about the development of the information and the selection of genes. The findings indicated that the methodology is 95.45% reliable on the cancer database. Refs. [8,9] presented a method of classifying ALL in its subtypes and bone marrow reactive (normal) in bone marrow stained images. The model for bone marrow imagery trained using deep learning techniques (CNN) to generate reliable classification tests. Experimental results indicate 97.78% accuracy. Additionally, the authors claimed that the proposed method could be used as a tool to treat acute lymphoblastic leukemia and its subtypes to certainly support pathologists.

The strategy for the diagnosis of Leukaemia using Artificial Bee Colony (ABC) for the training of Back Propagation Neural Network (BPNN) proposed by Sharma and Kumar [105]. Initially, Principal Component Analysis (PCA) used to reduce the dimension of the initial Leukemia database. ABC also fits well with BPNN, as ABC algorithm aims to promote worldwide convergence. In this sense, ABC operates efficiently to gain an optimum feature set. Tests from the classification have shown that the average accuracy obtained by the ABCBPNN system is 98.72%. The findings reveal that the efficiency of the ABC-BPNN system based on PCA is higher than the GA-BPNN system based on PCA. The solution introduced decreases the estimation rates and increases overall device

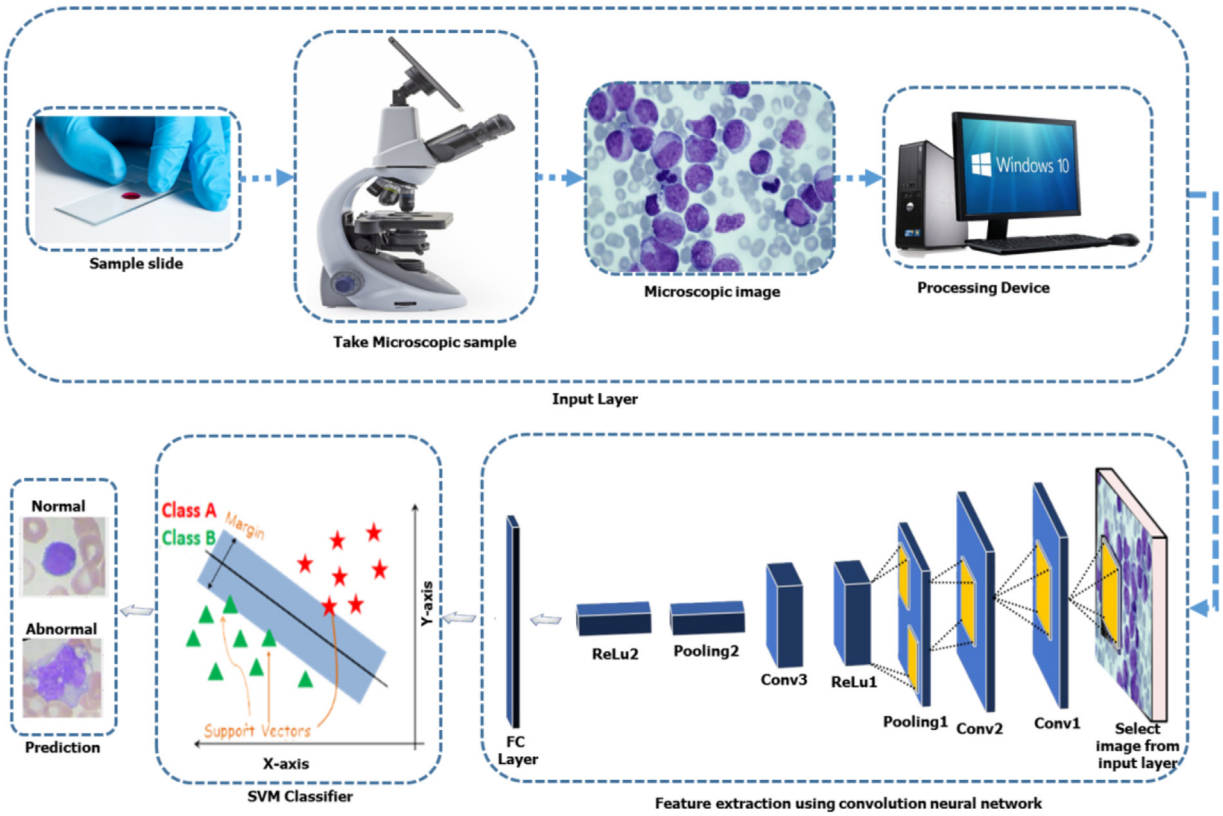

Fig. 5. Overview of ALL feature extraction and classification process for Leukemia detection.

performance. However, the experiments performed on a small dataset.

Zhang et al. [106] employed three techniques to assess the impact of the leukocyte category based on 5000 images obtained from a local hospital. Firstly, using CNN apps as the SVM input for classification of leukocytes, with 94.23% specificities, 95.10% specificity and 94.41% accuracy. Specificity, 87.50 % sensitivity and 85 % accuracy is obtained through the usage of the HOG features in the SVM program. The implementation of the standard characteristics CNN and HOG obtained 94.57%, 96.11%, and 95.93% precision. But they did not compare results in state of art. Rehman et al., [8] classified ALL into its subtypes and reactive bone marrow in stained bone marrow images. They proposed ST segmentation and deep learning techniques with the convolutional neural network are used to train the model on the bone marrow images. Classification results reported 97.78% accuracy. Table 4 includes a short overview, comparison of existing leukemia approaches, results, dataset.

Breast cancer

Breast Cancer occurs in the breast cells and is the most prevalent cancer in women in the world after skin cancer. Males and females both may suffer from breast cancer, but it is much more prevalent in females [108]. Machine assisted systems are not only the latest development in medical imaging for the initial finding of breast cancer but also enhances the diagnostic skill of radiologists. The most common tools employed for breast cancer diagnostics are mammography, tomography, Breast Ultrasound (BUS), MRI, CT scans and even more deeply PET is advised [109]. Typically, the breast is counted as the oversensitive organ of the human body, so only some of these procedures are advised, which depends upon the patient's condition and the tumor status. Mammography is considered a low-cost and secure procedure at an early stage of breast cancer, but it is ineffective in dense breast of young female. BUS procedure is considered supportive to mammograms [110] to prevent needless biopsy. Several datasets of breast imaging are publically available which are DDSM, MIAS, WBCD, BCDR and NBIA etc [111]. Following image acquisition, various operations of pre-processing are performed before segmentation such as pectoral muscle removal and artifacts removal etc. The process of segmentation is the most important step of the machine-assisted system for enhancing accuracy and to reduce false positive of the existence of abnormality [17]. Numerous studies recommended GLCM method to describe texture-based features [11,40,64]. Similarly, LBP is another remarkable mechanism used for texture extraction to isolate benign masses from malignant ones [112].

The diagnosis of breast cancer greatly depends upon the classification performance. Several machine learning approaches such as neural networks, decision trees, KNN, SVM and Ensemble classifiers are applied for the training and testing of features to distinguish the objects into a malignant or benign class [108,113]. To identify biased genes, Ref. [114] suggested a hybrid selection model. The issue with many groups is addressed with the aid of a decision tree classifier and the prediction of subtypes of breast cancer using the same or lesser number of genes is 100 % accurate.

The use of machine learning techniques is a breakthrough in life sciences particularly the use of deep learning architectures that have generated encouraging results. Currently, CNN has attracted researchers for breast tumor detection and classification. There are several CNN structural designs such as AlexNet, CiFarNet [115], GoogLeNet [116], VGG16 and VGG 19 [75,77]. Fig. 6 demonstrates deep learning architecture for breast cancer detection.

The input layer, output layer and other hidden layers in the Convolutional Neural Network architecture are completely linked layers known as transforming, pooling. Abdel-Zaher and Eldeib [117] proposed a CNN based method for the detection of breast car-

Table 4
Current methods, dataset and result for leukemia detection.

Reference	Methodology	Results (%)
	Deep Convolutional Neural Network	97.78%
Patel and Mishra, [103]	Used k-state grouping, histogram alignment, and the zack, SVM is used for classification	93.57 (Accuracy)
Kazemi et al., [107]	Used SVMs to classify acute myelogenous leukemia.	96% (Accuracy) 95% (sensitivity) 98% (specificity)
Khalilabad and Hassanpour, [104]	J48 Tree	95.45 (Accuracy)
Rehman et al., [5]	CNN using AlexNet architecture	97.78 (Accuracy)
Sharma and Kumar, [105]	PCA based ABCBPNN	98.7%(Accuracy) 0.478% (FAR) 0.398% (FRR)
Zhang et al., [106]	CNN features as the input of SVM for classification Combined CNN and HOG features	95.9% (Accuracy) 96.1% (sensitivity) 94.57% (specificity

SVM (Support Vector Machine), CNN (Convolution Neural Network), PCA (Principal Component Analysis), BPNN (Back-Propagation Neural Network), ABC (Artificial Bee Colony), ABCBPNN (Artificial Bee Colony Back-Propagation Neural Network), HOG (Histogram of the oriented gradient).

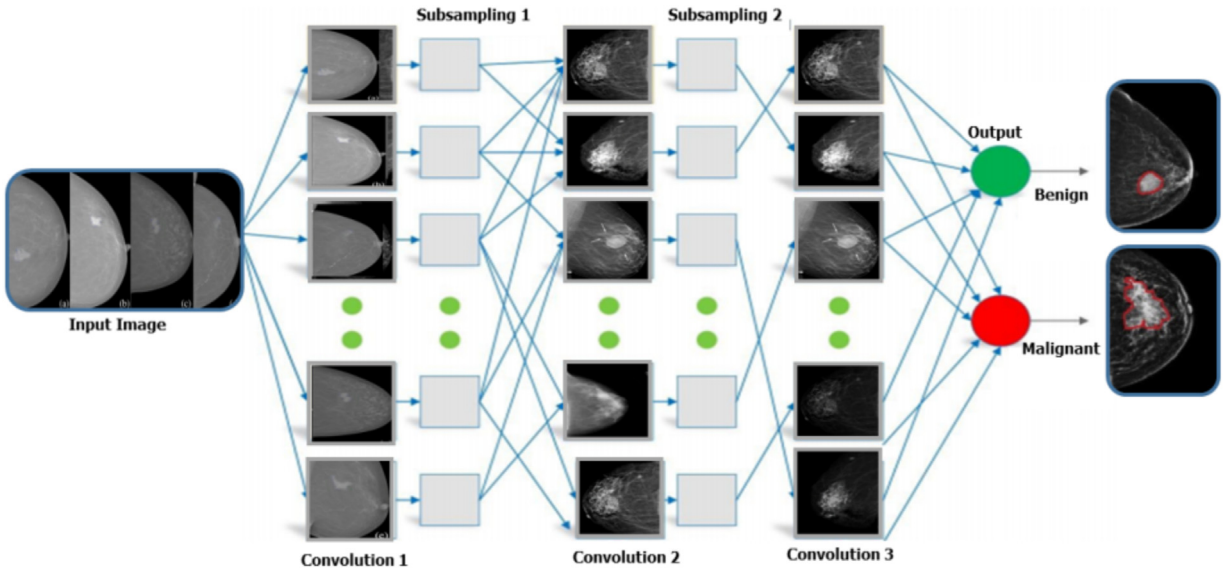

Fig. 6. Deep Convolutional Framework (DCNN) process for breast cancer detection.

cinoma utilizing an unmonitored pathway network of deep-faith beliefs accompanied by a backward propagation route. Wisconsin Breast Cancer Dataset (WBCD) employed for experiments and 99.68% accuracy claimed. Sun et al. [118] proposed a classification model for breast cancer. A graph-based semi-serviced learning (SSL) system was developed utilizing a deep convolutionary neural network (CNN). CNN typically uses significant quantities of labeled data for parameter training and fine-tuning, and only a limited portion of labeled data in the training set is expected from the proposed arrangements. The diagnostic device contained four modules: data measuring, collection of tasks, separation of data co-training and CNN. Their research included 3158 regions of interest (ROI), each with a size of 1874 mammographic pairs. Of these, 100 ROIs were viewed as identified data while the remainder were deemed unmarked. The region under the curve (AUC) of the sample was 0.8818, and for a combined marking and non-labeled results, the precision of CNN is 0.8243.

Inception V3 and Inception-ResNet V2 architectures were introduced by [119], and 90% of Tongji Hospital datasets were qualified and checked on the remaining 10% as well as the independent test collection. The models have been linked to the success of five radiologists. The performance of the models has been evaluated for accuracy, flexibility and specificity. In the estimation of the final diagnosis therapeutic of axillary node metastase in the independent test method, an AUC of 0.89 was obtained by the highest performing CNN, iteration V3. 85% responsiveness and 73% characteristics were obtained in this model. However, they did not compare results in state of art. Acharya et al. [120] employed deep understanding, K-means, autoencoder, and enhanced loss feature (ELF) in the classification to handle diagnostic errors via the enhancement of image quality and processing time based on five data sets, histopathological images were taken and pre-treated using a linear transformation filter and stain normalization. Such images have been fixed in sizes of 512 €/512 and 128 € /128 € and processed such that relevant knowledge on the images is accessible on the tissue and cell rates. ResNet 50-128 and ResNet512 were both pre-trained for the patches. The 128/128 were clustered and auto-encoders were used to achieve better cluster results using K-means, which employed a latent image feature. The SVM loss function and optimization problem were merged. The algorithm for deep learning has improved the precision of the breast cancer diagnosis to 97%, and but processing time exceeded from 30 to 40 s. Table 5 exhibits a brief description and comparison of current reported techniques, results, datasets for breast cancer.

Table 5
Current methods, dataset and result for breast cancer detection.

Reference	Methodology	Dataset	Results (%)
Abdel-Zaher and Eldeib, [117]	Deep belief network unsupervised path followed by backpropagation supervised path	WBCD	99.68 (Accuracy) 100 (sensitivity) 99.47 (specificity)
Sun et al., [118]	Semi-supervised learning with Convolution neural network	FFDM	82.43 (Accuracy) 81.00 (sensitivity) 72.26 (specificity)
Sadad et al., [108]	Fuzzy C-Means and region-growing based technique for segmentation, LBP-GLCM and LPQ technique used for feature extraction	MIAS -------- DDSM	97.2 (Accuracy) 97 (Specificity) 98 (Sensitivity) 97 (F-Score) 94 (MCC) ---------- 94.4 (Accuracy) 92 (Specificity) 96 (Sensitivity) 96 (F-Score) 88 (MCC)
Mughal et al., [16]	discrete differentiation operator, detect the edges boundaries and Convex hull technique	CEDM MIAS	3.51 ± 1.58 (Hausdorff Distance (HD)) 0.98 (FP-mean) 5.66 (FN mean) 3.52 ± 1.59 (Hausdorff Distance (HD)) 0.99 (FP-mean) 5.67 (FN mean)
Mughal et al., [19]	Morphological and Textural operators	DDSM MIAS	97 (Accuracy) 98 (Accuracy)
Mughal et al., [17]	Combination of HAT transformation with GLCM	MIAS DDSM	Benign:Malignant (MIAS) 95.0 (Accuracy) 100 (Sensitivity) 90.0 (Sensitivity) 0.9551 (AUC) Benign: Malignant (DDSM) 98.0 (Accuracy) 100 (Sensitivity) 93.0 (Sensitivity) 0.9876 (AUC)
Duarte et al., [121]	Texture features and Fisher discriminant analysis	MIAS	13 texture features 94.5 ± 0.019 (AUC) 5 texture features 0.884 ± 0.025 (AUC)
Vijayarajeswari et al., [113]	Support Vector Machine	MIAS	94 (Accuracy)
Zhou et al., [119]	Inception V3, Inception-ResNet V2, and ResNet-101	Tongji Hospital dataset	0.89 (AUC) 85% sensitivity 73% specificity
Acharya et al., [120]	K-means, autoencoder, ResNet50-128, ResNet512 and ELF	BI-RADS	97 (Accuracy)

WBCD (Wisconsin Breast Cancer Dataset) LBP-GLCM (local binary pattern grey level co-occurrence matrix), LPQ (Local Phase Quantization), SVM (Support Vector Machine), MCC (Matthews's correlation coefficient), AUC (area under the curve), FFDM (full-field digital mammography), ELF (enhanced loss function).

Liver cancer

Most scientists used machine learning methods to identify tumors in the liver [122]. Three characteristics used by automatic systems utilizing multiple-step CT images, namely form, shape and kinetic curves. Hamm et al. [123], used CNN design used multiphasic MRI and obtained an integrated process focused on CNNs for CT image section accidents [124]. The researchers contrasted the CNN models with common algorithms for machine learning: AdaBoost, RF and SVM. Such classifiers were designed with mean, variation, and contextual characteristics. The average coefficient of dice comparisons (DSC), precision and alerts hit 80.06% ± 1.63%, 82.67% ± 1.43%, and 84.34% ± 1.61% respectively. The findings suggest that the CNN approach performs well than other approaches and is promising for the segmentation of liver tumors. The efficiency and contrast of AdaBoos, RF, SVM experimented on a fairly limited dataset.

A BoVW approach to describe Focal Liver Injuries (FLLs) was proposed by Xu et al., [137]. The region of interest (ROI) pixels defined using the rotative invariant standardized local binary pattern system in nine texture groups. Therefore, a method of describing the spatial cone matching (SCM) introduced to explain the spatial details for the ROI's visual terms. Frid-Adar et al., [130] suggested the usage of recently introduced deeper learning methods for synthetic medical image generation (GAN) to improve the efficiency of CNN for the classification of medical image. A small data collection of CT images of 182 liver lesions illustrated the proposed procedure. GAN architectures were first used to synthesize good quality ROI liver lesions. Then a new method for the diagnosis of liver lesions with CNN was introduced. The efficiency of classification using classic data raises yielded 78.6% responsiveness and 88.4% specificity. The findings improved to 85.7% responsiveness and 92.4% accuracy after incorporating the synthesized data rise.

Romero et al. [125] suggested an end-to-end solution to deep learning to promote differentiation between colorectal liver metastases and healthy cysts in the liver's CT images. In this method, the effective extraction function InceptionV3 is implemented in conjunction with the residual ties and pre-trained ImageNet weights.

Table 6
Current methods, dataset and result for liver cancer detection.

Reference	Methodology	Modality	Results (%)
Li, [124]	CNN, Adaboost, RF, SVM	CT	80.06 (DSC) 82.67 (precision) 84.34 (recall)
Ben-Cohen et al., [129]	Fully convolutional network (FCN)	CT	0.86 (true positive rate) 0.6 (false positive per case)
Chang et al., [122]	texture, shape, and kinetic curve and logistic regression analysis was used for classification	CT	81.69 (Accuracy) 81.82 (sensitivity) 81.63 (specificity)
Xu et al., [137]	BoVW-feature and rotation-invariant uniform local binary pattern	CT	80 (Accuracy)
Frid-Adar et al., [130]	GAN for data augmentation and CNN for classification	CT	85.7(sensitivity) 92.4(specificity)
Jansen et al., [127]	Contrast curve, gray level histogram, GLCM	MRI	77 (Accuracy) 0.79 (average sensitivity) 0.77 (average specificity)
Hamm et al., [123]	Convolution neural network (CNN)	MRI	92 (Accuracy) 92 (sensitivity) 98 (specificity) 93.5 (true positive) 1.6 (false positive)
Romero et al., [125]	Inception V3 + Deep learning	CT	96 (Accuracy) 0.92 (F1-score) 0.97 (AUC) 1.00 (Precision) 0.94 (Recall) 0.85(Specificity)
Parsai et al., [126]	Merged features based on MRI/PET/CT	CT/PET/MRI	94.7 (Accuracy) 91.9 (sensitivity) 97.4 (specificity) 97.1 (PPV) 92.5 (NPV)
Schmauch et al., [131]	Deep Learning	US	93 (Accuracy) 0.891 (AUC scores)
Ben-Cohen and Greenspan, [128]	FCN with the conditional generative adversarial network (GAN)	CT/PET	90.9 (TPR) 3.0 (FPC)

CNN (Convolution Neural Network), SVM (Support Vector Machine), RF (Radom Forecast), FCN (Fully Convolutional Network), BoVW (Bag of Visual Words), CT (Computed Tomography), GAN (Generative Adversarial Networks), GLCM (grey level co-occurrence matrix), DSC (dice similarity coefficient), AUC (Area Under the Curve), PET (Positron Emission Tomography), MRI (Magnetic Resonance Imaging) PPV (Positive Predictive Values) NPV (Negative Predictive Values).

The architecture also consists of completely linked classification layers to generate a probabilistic lesion style production. They used a surgical biobank in-house of 230 liver lesions from 63 patients. The accuracy 0.96% and F1 0.92% claimed without specifying experimental setup and no benchmark dataset employed. The approach suggested by PET / CT and MRI for the elimination of contrast gradient, gray level histogram and gray-level co-occurring of liver lesions. Parsai et al. [126] demonstrated as a feasible and effective strategy to enhance the identification and characterization of FDG PET / CT and FDG liver damages that remain indeterminate after liver RMI / CT. Jansen et al. [127] used external factors such as the involvement of steatosis, cirrhosis, reported primary tumor that identified as characteristics. Fifty ANOVA F-score attributes have been picked and fed to a rather random tree grouping. The classifier testing was performed using the leave-out theory and ROC (ROC) curve study. Ben-Cohen and Greenspan [128] proposed a modern method, a modern method to produce realistic PET images by utilizing CT scans, integrating the FCN with a GAN to create digital PET information from input CT information, which reveals its advantage by its false-positive rate. Table 6 summarizes existing approaches for liver cancer using machine learning, results, and datasets.

Conclusion and challenges

The past few decades are witnessed a revolution in detection and cure of cancer using machines assistance. Accordingly, this paper has presented a systematic review of current techniques in diagnosis and cure of several cancers affecting human body badly. The focus of this article is to review, analyze, categorize methodologies of different types of cancer and uncover existing limitations. The review has presented six types of cancers lung cancer, breast cancer, brain tumor, liver cancer, leukemia, and skin cancer. Additionally, this study has presented four significant stages of automated cancer diagnosis such as image pre-processing, tumor segmentation, feature extraction, and classification using benchmark datasets. The primary intention of this research is to present an intelligent background to new researchers who wish to begin their research activity in this field.

To conclude, a systematic review of the current state of art machine assisted cancer detection techniques along with their pros and cons. However, still accuracy for each cancer category is far from maturity. Most of the researchers either did not employ benchmark datasets or used small sets for testing of their proposed techniques. For this purpose, the current state of art techniques are compared on benchmark datasets and limitations of existing techniques are highlighted.

Main challenges in the cancer detection and cure process are redesign research pipeline, understand the cancer growth phenomena, develop preclinical models, handling complex cancers precisely, early treatment, innovative methods of designing and delivering clinical trials and enhance accuracy that will be useful for the physicians as a second and early opinion.

Funding

This work funded by the research Project [Brain Tumor Detection and Classification using 3D CNN and Feature Selection Architecture]; Prince Sultan University; Saudi Arabia [SEED-CCIS-2020{30}].

Acknowledgements

This work was supported by the research Project [Brain Tumor Detection and Classification using 3D CNN and Feature Selection Architecture]; Prince Sultan University; Saudi Arabia [SEED-CCIS-2020{30}]. Additionally author is thankful to the anonymous reviewers for their constructive comments and apologize to those researchers whom work is overlooked in this research.

References

[1] Abbas N, Saba T, Mehmood Z, Rehman A, Islam N, Ahmed KT. An automated nuclei segmentation of leukocytes from microscopic digital images. Pak J Pharm Sci 2019;32(5):2123–38.
[2] Abbas N, Saba T, Rehman A, Mehmood Z, Javaid N, Tahir M, et al. Plasmodium species aware based quantification of malaria, parasitemia in light microscopy thin blood smear. Microsc Res Tech 2019;82(July (7)):1198–214, http://dx.doi.org/10.1002/jemt.23269.
[3] Abbas N, Saba T, Rehman A, Mehmood Z, kolivand H, Uddin M, et al. Plasmodium life cycle stage classification based quantification of malaria parasitaemia in thin blood smears. Microsc Res Tech 2018, doi.org/10.1002/jemt.23170.
[4] Abbas N, Saba T, Mohamad D, Rehman A, Almazyad AS, Al-Ghamdi JS. Machine aided malaria parasitemia detection in Giemsa-stained thin blood smears. Neural Comput Appl 2018;29(3):803–18, http://dx.doi.org/10.1007/s00521-016-2474-6.
[5] Rehman A, Abbas N, Saba T, Rahman SIU, Mehmood Z, Kolivand K. Classification of acute lymphoblastic leukemia using deep learning. Microsc Res Tech 2018;81(11):1310–7, http://dx.doi.org/10.1002/jemt.23139.
[6] Rehman A, Abbas N, Saba T, Mehmood Z, Mahmood T, Ahmed KT. Microscopic malaria parasitemia diagnosis and grading on benchmark datasets. Microscopic Research and Technique 2018;81(9):1042–58, http://dx.doi.org/10.1002/jemt.23071.
[7] Rehman A, Abbas N, Saba T, Mahmood T, Kolivand H. Rouleaux red blood cells splitting in microscopic thin blood smear images via local maxima, circles drawing, and mapping with original RBCs. Microscopic research and technique 2018;81(7):737–44, http://dx.doi.org/10.1002/jemt.23030.
[8] Amin J, Sharif M, Raza M, Saba T, Anjum MA. Brain tumor detection using statistical and machine learning method. Comput Methods Programs Biomed 2019;177:69–79.
[9] Amin J, Sharif M, Raza M, Saba T, Rehman A. Brain tumor classification: feature fusion. In: 2019 International Conference on Computer and Information Sciences (ICCIS). 2019. p. 1–6.
[10] Saba T, Khan MA, Rehman A, et al. Region extraction and classification of skin Cancer: a heterogeneous framework of deep CNN features fusion and reduction. J Med Syst 2019;43:289, http://dx.doi.org/10.1007/s10916-019-1413-3.
[11] Saba T, Khan SU, Islam N, Abbas N, Rehman A, Javaid N, et al. Cloud based decision support system for the detection and classification of malignant cells in breast cancer using breast cytology images. Microsc Res Tech 2019;82(6):775–85.
[12] Saba T, Sameh A, Khan F, Shad SA, Sharif M. Lung nodule detection based on ensemble of hand crafted and deep features. J Med Syst 2019;43(12):332.
[13] Iqbal S, Khan MUG, Saba T, Rehman A. Computer assisted brain tumor type discrimination using magnetic resonance imaging features. Biomed Eng Lett 2017;8(1):5–28, http://dx.doi.org/10.1007/s13534-017-0050-3.
[14] Iqbal S, Ghani MU, Saba T, Rehman A. Brain tumor segmentation in multispectral MRI using convolutional neural networks (CNN). Microsc Res Tech 2018;81(4):419–27.
[15] Amin J, Sharif M, Yasmin M, Saba T, Raza M. Use of machine intelligence to conduct analysis of human brain data for detection of abnormalities in its cognitive functions. Multimed Tools Appl 2019;2019, http://dx.doi.org/10.1007/s11042-019-7324-y.
[16] Mughal B, Muhammad N, Sharif M, Rehman A, Saba T. Removal of pectoral muscle based on topographic map and shape-shifting silhouette. BMC Cancer 2018;18:778.
[17] Mughal B, Sharif M, Muhammad N, Saba T. A novel classification scheme to decline the mortality rate among women due to breast tumor. Microsc Res Tech 2018;81:171–80.
[18] Amin J, Sharif M, Raza M, Saba T, Sial R, Shad SA. Brain tumor detection: a long short-term memory (LSTM)-based learning model. Neural Comput Appl 2019:1–9.
[19] Mughal B, Muhammad N, Sharif M, Saba T, Rehman A. Extraction of breast border and removal of pectoral muscle in wavelet, domain. Biomed Res 2017;28(11):5041–3.
[20] Khan MA, Lali IU, Rehman A, Ishaq M, Sharif M, Saba T, et al. Brain tumor detection and classification: A framework of marker-based watershed algorithm and multilevel priority features selection. Microsc Res Tech 2019, http://dx.doi.org/10.1002/jemt.23238.
[21] Khan SA, Nazir M, Khan MA, Saba T, Javed K, Rehman A, et al. Lungs nodule detection framework from computed tomography images using support vector machine. Microsc Res Tech 2019, http://dx.doi.org/10.1002/jemt.23275.
[22] Khan MA, Akram T, Sharif M, Saba T, Javed K, Lali IU, et al. Construction of saliency map and hybrid set of features for efficient segmentation and classification of skin lesion. Microsc Res Tech 2019, http://dx.doi.org/10.1002/jemt.23220.
[23] Khan MQ, Hussain A, Rehman SU, Khan U, Maqsood M, Mehmood K, et al. Classification of melanoma and nevus in digital images for diagnosis of skin Cancer. IEEE Access 2019;7:90132–44.
[24] Javed R, Rahim MSM, Saba T, Rehman A. A comparative study of features selection for skin lesion detection from dermoscopic images. Netw Model Anal Health Inform Bioinform 2020;9(1):4.
[25] Javed R, Saba T, Shafry M, Rahim M. An intelligent saliency segmentation technique and classification of Low contrast skin lesion dermoscopic images based on histogram decision. In: 2019 12th International Conference on Developments in Esystems Engineering (DeSE). 2020. p. 164–9.
[26] Javed R, Rahim MSM, Saba T, Rashid M. Region-based active contour JSEG fusion technique for skin lesion segmentation from dermoscopic images. Biomed Res 2019;30(6):1–10.
[27] Ullah H, Saba T, Islam N, Abbas N, Rehman A, Mehmood Z, et al. An ensemble classification of exudates in color fundus images using an evolutionary algorithm based optimal features selection. Microsc Res Tech 2019, http://dx.doi.org/10.1002/jemt.23178.
[28] Jamal A, Hazim Alkawaz M, Rehman A, Saba T. Retinal imaging analysis based on vessel detection. Microsc Res Tech 2017;80(17):799–811, http://dx.doi.org/10.1002/jemt.
[29] Saba T, Bokhari STF, Sharif M, Yasmin M, Raza M. Fundus image classification methods for the detection of glaucoma: A review. Microsc Res Tech 2018, http://dx.doi.org/10.1002/jemt.23094.
[30] Fahad HM, Khan MUG, Saba T, Rehman A, Iqbal S. Microscopic abnormality classification of cardiac murmurs using ANFIS and HMM. Microsc Res Tech 2018;81(5):449–57, http://dx.doi.org/10.1002/jemt.22998.
[31] Bray F, Ferlay J, Soerjomataram I, Siegel RL, Torre LA, Jemal A. Global cancer statistics 2018: GLOBOCAN estimates of incidence and mortality worldwide for 36 cancers in 185 countries. CA Cancer J Clin 2018;68:394–424.
[32] Kurihara Y, Matsuoka S, Yamashiro T, Fujikawa A, Matsushita S, Yagihashi K, et al. MRI of pulmonary nodules. Am J Roentgenol 2014;202:W210–6.
[33] White C. New techniques in thoracic imaging. CRC Press; 2001.
[34] [Accessed by 2014]. Breast Cancer Surveillance Consortium. https://www.bcsc-research.org/data/mammography_dataset.
[35] Iftikhar S, Fatima K, Rehman A, Almazyad AS, Saba T. An evolution based hybrid approach for heart diseases classification and associated risk factors identification. Biomed Res 2017;28(8):3451–5.
[36] Liaqat A, Khan MA, Sharif M, Mittal M, Saba T, Manic KS, et al. Gastric Tract Infections Detection and Classification from Wireless Capsule Endoscopy using Computer Vision Techniques: A Review. Curr Med Imaging Rev 2020.
[37] Al-Ameen Z, Sulong G, Rehman A, Al-Dhelaan A, Saba T, Al-Rodhaan M. An innovative technique for contrast enhancement of computed tomography images using normalized gamma-corrected contrast-limited adaptive histogram equalization. EURASIP J Adv Signal Process 2015:32, http://dx.doi.org/10.1186/s13634-015-0214-1.
[38] Rahim MSM, Norouzi A, Rehman A, Saba T. 3D bones segmentation based on CT images visualization. Biomed Res 2017;28(8):3641–4.
[39] Rahim MSM, Rehman A, Kurniawan F, Saba T. Ear biometrics for human classification based on region features mining. Biomed Res 2017;28(10):4660–4.
[40] Yousaf K, Mehmood Z, Saba T, Rehman A, Munshi AM, Alharbey R, et al. Mobile-health applications for the efficient delivery of health care facility to people with dementia (PwD) and support to their carers: a survey. Biomed Res Int 2019;2019:1–26.
[41] Marie-Sainte SL, Aburahmah L, Almohaini R, Saba T. Current techniques for diabetes prediction: review and case study. Appl Sci 2019;9(21):4604.
[42] Marie-Sainte SL, Saba T, Alsaleh D, Alotaibi A, Bin M. An improved strategy for predicting diagnosis, survivability, and recurrence of breast Cancer. J Comput Theor Nanosci 2019;16(9):3705–11.
[43] Ejaz K, Rahim MSM, Rehman A, Chaudhry H, Saba T, Ejaz A, et al. segmentation method for pathological brain tumor and accurate detection using MRI. Int J Adv Comput Sci Appl 2018;9(8):394–401.
[44] Tahir B, Iqbal S, Khan MUG, Saba T, Mehmood Z, Anjum A, et al. Feature enhancement framework for brain tumor segmentation and classification. Microsc Res Tech 2019, http://dx.doi.org/10.1002/jemt.23224.
[45] Husham A, Alkawaz MH, Saba T, Rehman A, Alghamdi JS. Automated nuclei segmentation of malignant using level sets. Microsc Res Tech 2016;79(10):93–97, http://dx.doi.org/10.1002/jemt.22733.
[46] Saba T. Automated lung nodule detection and classification based on multiple classifiers voting. Microsc Res Tech 2019;2019:1–9, http://dx.doi.org/10.1002/jemt.23326.

[47] Mittal A, Kumar D, Mittal M, Saba T, Abunadi I, Rehman A, et al. Detecting pneumonia using convolutions and dynamic capsule routing for chest X-ray images. Sensors 2020;20(4):1068.
[48] American Cancer Society. C.D.O.P.H., California Cancer registry 2017. California Cancer facts & figures; 2017.
[49] Khan MA, Sharif MI, Raza M, Anjum A, Saba T, Shad SA. Skin lesion segmentation and classification: A unified framework of deep neural network features fusion and selection. Expert Syst 2019:e12497.
[50] Khan MW, Sharif M, Yasmin M, Saba T. CDR based glaucoma detection using fundus images: a review. Int J Appl Pattern Recogn 2019;4(3):261–306.
[51] Javed R, Rahim MSM, Saba T. An improved framework by mapping salient features for skin lesion detection and classification using the optimized hybrid features. Int J Adv Trends Comput Sci Eng 2019;8(1):95–101.
[52] Torre LA, Trabert B, Desantis CE, Miller KD, Samimi G, Runowicz CD, et al. Ovarian cancer statistics, 2018. CA Cancer J Clin 2018;68:284–96.
[53] Abbas N, Mohamad D, Abdullah AH, Saba T, Al-Rodhaan M, Al-Dhelaan A. Nuclei segmentation of leukocytes in blood smear digital images. Pak J Pharm Sci 2015;28(5):1801–6.
[54] Norouzi A, Rahim MSM, Altameem A, Saba T, Rada AE, Rehman A, et al. Medical image segmentation methods, algorithms, and applications. Iete Tech Rev 2014;31(3):199–213, http://dx.doi.org/10.1080/02564602.2014.906861.
[55] Stewart B, Wild CP. World cancer report; 2014. p. 2014.
[56] Perveen S, Shahbaz M, Saba T, Keshavjee K, Rehman A, Guergachi A. Handling irregularly sampled longitudinal data and prognostic modeling of diabetes using machine learning technique. IEEE Access 2020;8:21875–85.
[57] Bareiro Paniagua LR, Leguizamón Correa DN, Pinto-Roa DP, Vázquez Noguera JL, Toledo S, Lizza A. Computerized medical diagnosis of melanocytic lesions based on the ABCD approach. Clei Electron J 2016;19, 6-6.
[58] Ramzan F, Khan MUG, Rehmat A, Iqbal S, Saba T, Rehman A, et al. A deep learning approach for automated diagnosis and multi-class classification of alzheimer's disease stages using resting-state fMRI and residual neural networks. J Med Syst 2020;44(2):37.
[59] Lu Z, Bai Y, Chen Y, Su C, Lu S, Zhan T, et al. The classification of gliomas based on a pyramid dilated convolution ResNet model. Pattern Recognit Lett 2020.
[60] Nayak DR, Dash R, Majhi B, Pachori RB, Zhang Y. A deep stacked random vector functional link network autoencoder for diagnosis of brain abnormalities and breast cancer. Biomed Signal Process Control 2020;58:101860.
[61] Nayak DR, Dash R, Majhi B. Automated diagnosis of multi-class brain abnormalities using MRI images: a deep convolutional neural network based method. Pattern Recognit Lett 2020.
[62] Qureshi I, Khan MA, Sharif M, Saba T, Ma J. Detection of glaucoma based on cup-to-disc ratio using fundus images. Int J Intell Syst Technol Appl 2020;19(1):1–16, http://dx.doi.org/10.1504/IJISTA.2020.105172.
[63] Nazir M, Khan MA, Saba T, Rehman A. Brain tumor detection from MRI images using multi-level wavelets. 2019, IEEE International Conference on Computer and Information Sciences (ICCIS) 2019:1–5.
[64] Khan S, Islam N, Jan Z, Din IU, Rodrigues JJC. A novel deep learning based framework for the detection and classification of breast cancer using transfer learning. Pattern Recognit Lett 2019;125:1–6.
[65] Khan MA, Sharif M, Akram T, Raza M, Saba T, Rehman A. Hand-crafted and deep convolutional neural network features fusion and selection strategy: an application to intelligent human action recognition. Appl Soft Comput 2020;87:105986.
[66] Vaishnavee K, Amshakala K. An automated MRI brain image segmentation and tumor detection using SOM-clustering and proximal support vector machine classifier. In: 2015 IEEE International Conference on Engineering and Technology (ICETECH). 2015. p. 1–6.
[67] Ellwaa A, Hussein A, Alnaggar E, Zidan M, Zaki M, Ismail MA, et al. Brain tumor segmantation using random forest trained on iteratively selected patients. International Workshop on Brainlesion: Glioma, Multiple Sclerosis, Stroke and Traumatic Brain Injuries 2016:129–37.
[68] Nie D, Zhang H, Adeli E, Liu L, Shen D. 3D deep learning for multi-modal imaging-guided survival time prediction of brain tumor patients. In: International Conference on Medical Image Computing and Computer-Assisted Intervention. 2016. p. 212–20.
[69] Wasule V, Sonar P. Classification of brain MRI using SVM and KNN classifier. In: 2017 Third International Conference on Sensing, Signal Processing and Security (ICSSS). 2017. p. 218–23.
[70] Fidon L, Li W, Garcia-Peraza-Herrera LC, Ekanayake J, Kitchen N, Ourselin S, et al. Scalable multimodal convolutional networks for brain tumour segmentation. International Conference on Medical Image Computing and Computer-Assisted Intervention 2017:285–93.
[71] Abbasi S, Tajeripour F. Detection of brain tumor in 3D MRI images using local binary patterns and histogram orientation gradient. Neurocomputing 2017;219:526–35.
[72] Iqbal S, Ghani Khan MU, Saba T, Mehmood Z, Javaid N, Rehman A, et al. Deep learning model integrating features and novel classifiers fusion for brain tumor segmentation. Microsc Res Tech 2019;82:1302–15.
[73] Mehmood I, Sajjad M, Muhammad K, Shah SIA, Sangaiah AK, Shoaib M, et al. An efficient computerized decision support system for the analysis and 3D visualization of brain tumor. Multimed Tools Appl 2019;78:12723–48.
[74] Das D, Mahanta LB, Ahmed S, Baishya BK, Haque I. Automated classification of childhood brain tumours based on texture feature. Songklanakarin Journal of Science & Technology 2019:41.
[75] Saba T, Mohamed AS, El-Affendi M, Amin J, Sharif M. Brain tumor detection using fusion of hand crafted and deep learning features. Cogn Syst Res 2020;59:221–30.
[76] Arikan M, Fröhler B, Möller T. Semi-automatic brain tumor segmentation using support vector machines and interactive seed selection. Proceedings MICCAI-BRATS Workshop 2016:1–3.
[77] Ejaz K, Rahim MSM, Bajwa UI, Rana N, Rehman A. An unsupervised learning with feature approach for brain tumor segmentation using magnetic resonance imaging. Proceedings of the 2019 9th International Conference on Bioscience, Biochemistry and Bioinformatics 2019:1–7.
[78] Ramzan F, Khan MUG, Iqbal S, Saba T, Rehman A. Volumetric segmentation of brain regions from MRI scans using 3D convolutional neural networks. IEEE Access 2020;8:103697–709.
[79] Setio AAA, Ciompi F, Litjens G, Gerke P, Jacobs C, Van Riel SJ, et al. Pulmonary nodule detection in CT images: false positive reduction using multi-view convolutional networks. IEEE Trans Med Imaging 2016;35:1160–9.
[80] Dou Q, Chen H, Yu L, Qin J, Heng PA. Multilevel contextual 3-D CNNs for false positive reduction in pulmonary nodule detection. IEEE Trans Biomed Eng 2016;64:1558–67.
[81] Shen W, Zhou M, Yang F, Yu D, Dong D, Yang C, et al. Multi-crop convolutional neural networks for lung nodule malignancy suspiciousness classification. Pattern Recognit 2017;61:663–73.
[82] Van-Griethuysen JJ, Fedorov A, Parmar C, Hosny A, Aucoin N, Narayan V, et al. Computational radiomics system to decode the radiographic phenotype. Cancer Res 2017;77:e104–7.
[83] Tahoces PG, Alvarez L, González E, Cuenca C, Trujillo A, Santana-Cedrés D, et al. Automatic estimation of the aortic lumen geometry by ellipse tracking. Int J Comput Assist Radiol Surg 2019;14:345–55.
[84] Jiang H, Ma H, Qian W, Gao M, Li Y, Hongyang J, et al. An Automatic Detection System of Lung Nodule Based on Multigroup Patch-Based Deep Learning Network. IEEE J Biomed Health Inform 2018;22:1227.
[85] Naqi SM, Sharif M, Jaffar A. Lung nodule detection and classification based on geometric fit in parametric form and deep learning. Neural Comput Appl 2018:1–19.
[86] Naqi SM, Sharif M, Lali IU. A 3D nodule candidate detection method supported by hybrid features to reduce false positives in lung nodule detection. Multimed Tools Appl 2019;78:26287–311.
[87] Asuntha A, Srinivasan A. Deep learning for lung Cancer detection and classification. Multimed Tools Appl 2020:1–32.
[88] Shen W, Zhou M, Yang F, Yang C, Tian J. Multi-scale convolutional neural networks for lung nodule classification. In: International Conference on Information Processing in Medical Imaging. 2015. p. 588–99.
[89] Kumar D, Wong A, Clausi DA. Lung nodule classification using deep features in CT images. In: 2015 12th Conference on Computer and Robot Vision. 2015. p. 133–8.
[90] Firmino M, Angelo G, Morais H, Dantas MR, Valentim R. Computer-aided detection (CADe) and diagnosis (CADx) system for lung cancer with likelihood of malignancy. Biomed Eng Online 2016;15:2.
[91] Barata C, Celebi ME, Marques JS. A survey of feature extraction in dermoscopy image analysis of skin cancer. IEEE J Biomed Health Inform 2018;23(3):1096–109.
[92] Saba T, Al-Zahrani S, Rehman A. Expert system for offline clinical guidelines and treatment. Life Sci Journal 2012;9(4):2639–58.
[93] Ramya VJ, Navarajan J, Prathipa R, Kumar LA. Detection of melanoma skin cancer using digital camera images. ARPN Journal of Engineering and Applied Sciences 2015;10:3082–5.
[94] Premaladha J, Ravichandran K. Novel approaches for diagnosing melanoma skin lesions through supervised and deep learning algorithms. J Med Syst 2016;40:96.
[95] Aima A, Sharma AK. Predictive approach for melanoma skin Cancer detection using CNN. Ssrn Electron J 2019. Available at SSRN 3352407.
[96] Dai X, Spasić I, Meyer B, Chapman S, Andres F. Machine learning on mobile: an on-device inference app for skin cancer detection. In: 2019 Fourth International Conference on Fog and Mobile Edge Computing (FMEC). 2019. p. 301–5.
[97] Arthur F, Hossein KR. Deep learning in medical image analysis: a third eye for doctors. J Stomatol Oral Maxillofac Surg 2019.
[98] Li Y, Shen L. Skin lesion analysis towards melanoma detection using deep learning network. Sensors 2018;18:556.
[99] Rawat J, Bhadauria H, Singh A, Virmani J. Review of leukocyte classification techniques for microscopic blood images. Computing for sustainable global development (INDIACom). In: 2015 2nd International Conference on. 2015. p. 1948–54.
[100] Ramoser H, Laurain V, Bischof H, Ecker R. Leukocyte segmentation and classification in blood-smear images. Engineering in medicine and biology society, 2005. In: IEEE-EMBS 2005. 27th Annual International Conference of the. 2006. p. 3371–4.
[101] Su MC, Cheng CY, Wang PC. A neural-network-based approach to white blood cell classification. Sci World J 2014:2014.
[102] Putzu L, Di Ruberto C. White blood cells identification and counting from microscopic blood image. In: Proceedings of World Academy of Science, Engineering and Technology. 2013. p. 363.
[103] Patel N, Mishra A. Automated leukaemia detection using microscopic images. Procedia Comput Sci 2015;58:635–42.

[104] Khalilabad ND, Hassanpour H. Employing image processing techniques for cancer detection using microarray images. Comput Biol Med 2017;81:139–47.
[105] Sharma R, Kumar R. A novel approach for the classification of leukemia using artificial Bee Colony optimization technique and back-propagation neural networks. Proceedings of 2nd International Conference on Communication, Computing and Networking 2019:685–94.
[106] Zhang C, Wu S, Lu Z, Shen Y, Wang J, Huang P, et al. Hybrid Adversarial-Discriminative Network for Leukocyte Classification in Leukemia. Med Phys 2020.
[107] Kazemi F, Najafabadi TA, Araabi BN. Automatic recognition of acute myelogenous leukemia in blood microscopic images using K-means clustering and support vector machine. J Med Signals Sens 2016;6:183.
[108] Sadad T, Munir A, Saba T, Hussain A. Fuzzy C-means and region growing based classification of tumor from mammograms using hybrid texture feature. J Comput Sci 2018;29:34–45.
[109] Kumar A, Singh SK, Saxena S, Lakshmanan K, Sangaiah AK, Chauhan H, et al. Deep feature learning for histopathological image classification of canine mammary tumors and human breast cancer. Inf Sci (Ny) 2020;508:405–21.
[110] Kelly KM, Dean J, Comulada WS, Lee SJ. Breast cancer detection using automated whole breast ultrasound and mammography in radiographically dense breasts. Eur Radiol 2010;20:734–42.
[111] Dora L, Agrawal S, Panda R, Abraham A. Optimal breast cancer classification using Gauss–Newton representation based algorithm. Expert Syst Appl 2017;85:134–45.
[112] Rabidas R, Midya A, Chakraborty J, Arif WA. Study of different texture features based on local operator for benign-malignant mass classification. 6th International Conference On Advances In Computing & Communications, Procedia Computer Science 2016:389–95.
[113] Vijayarajeswari R, Parthasarathy P, Vivekanandan S, Basha AA. Classification of mammogram for early detection of breast cancer using SVM classifier and Hough transform. Measurement 2019;146:800–5.
[114] Etemadi R, Alkhateeb A, Rezaeian I, Rueda L. Identification of discriminative genes for predicting breast cancer subtypes. IEEE International Conference on Bioinformatics and Biomedicine (BIBM) 2016:1184–8, http://dx.doi.org/10.1109/bibm.2016.7822688.
[115] Roth H, Lu L, Liu J, Yao J, Seff A, Cherry K, et al. Improving computer-aided detection using convolutional neural networks and random view aggregation. IEEE Trans Med Imaging 2016;35:1170.
[116] Szegedy C, Liu W, Jia Y, Sermanet P, Reed S, Anguelov D, et al. Going deeper with convolutions. Proceedings of the IEEE Conference on Computer Vision and Pattern Recognition 2015:1–9.
[117] Abdel-Zaher AM, Eldeib AM. Breast cancer classification using deep belief networks. Expert Syst Appl 2016;46:139–44.
[118] Sun W, Tseng TLB, Zhang J, Qian W. Enhancing deep convolutional neural network scheme for breast cancer diagnosis with unlabeled data. Comput Med Imaging Graph 2017;57:4–9.
[119] Zhou LQ, Wu XL, Huang SY, Wu GG, Ye HR, Wei Q, et al. Lymph node metastasis prediction from primary breast cancer US images using deep learning. Radiology 2020;294:19–28.
[120] Acharya S, Alsadoon A, Prasad P, Abdullah S, Deva A. Deep convolutional network for breast cancer classification: enhanced loss function (ELF). J Supercomput 2020:1–18.
[121] Duarte MA, Pereira WC, Alvarenga AV. Calculating texture features from mammograms and evaluating their performance in classifying clusters of microcalcifications. Mediterranean Conference on Medical and Biological Engineering and Computing 2019:322–32.
[122] Chang CC, Chen HH, Chang YC, Yang MY, Lo CM, Ko WC, et al. Computer-aided diagnosis of liver tumors on computed tomography images. Comput Methods Programs Biomed 2017;145:45–51.
[123] Hamm CA, Wang CJ, Savic LJ, Ferrante M, Schobert I, Schlachter T, et al. Deep learning for liver tumor diagnosis part I: development of a convolutional neural network classifier for multi-phasic MRI. Eur Radiol 2019;29:3338–47.
[124] LI W. Automatic segmentation of liver tumor in CT images with deep convolutional neural networks. J Comput Commun 2015;3:146.
[125] Romero FP, Diler A, Bisson-Gregoire G, Turcotte S, Lapointe R, Vandenbroucke-Menu F, et al. End-to-End discriminative deep network for liver lesion classification. In: 2019 IEEE 16th International Symposium on Biomedical Imaging (ISBI 2019). 2019. p. 1243–6.
[126] Parsai A, Miquel ME, Jan H, Kastler A, Szyszko T, Zerizer I. Improving liver lesion characterisation using retrospective fusion of FDG PET/CT and MRI. Clin Imaging 2019;55:23–8.
[127] Jansen MJ, Kuijf HJ, Veldhuis WB, Wessels FJ, Viergever MA, Pluim JP. Automatic classification of focal liver lesions based on MRI and risk factors. PLoS One 2019:14.
[128] Ben-Cohen A, Greenspan H. Liver lesion detection in CT using deep learning techniques. Handbook of medical image computing and computer assisted intervention. Elsevier; 2020.
[129] Ben-Cohen A, Diamant I, Klang E, Amitai M, Greenspan H. Fully convolutional network for liver segmentation and lesions detection. Deep learning and data labeling for medical applications. Springer; 2016.
[130] Frid-Adar M, Diamant I, Klang E, Amitai M, Goldberger J, Greenspan H. GAN-based synthetic medical image augmentation for increased CNN performance in liver lesion classification. Neurocomputing 2018;321:321–31.
[131] Schmauch B, Herent P, Jehanno P, Dehaene O, Saillard C, Aubé C, et al. Diagnosis of focal liver lesions from ultrasound using deep learning. Diagn Interv Imaging 2019;100:227–33.
[132] Menze BH, et al. The multimodal brain tumor image segmentation benchmark (BRATS). IEEE Trans Med Imaging 2015;34(10):1993–2024.
[133] Xie H, Yang D, Sun N, Chen Z, Zhang Y. Automated pulmonary nodule detection in CT images using deep convolutional neural networks. Pattern Recogn 2019;85:109–19.
[134] Saba T, Haseeb K, Ahmed I, Rehman A, Saba T. Secure and energy-efficient framework using Internet of Medical Things for e-healthcare. J InfectPublic Health 2020, http://dx.doi.org/10.1016/j.jiph.2020.06.027.
[135] Saba T, Rehman A, Mehmood Z, Kolivand H, Sharif M. Image enhancement and segmentation techniques for detection of knee joint diseases: a survey. Curr Med Imaging Rev 2018;14(5), http://dx.doi.org/10.2174/1573405613666170912164546.
[136] Rehman A, Khan MA, Mehmood Z, Saba T, Sardaraz M, Rashid M. Microscopic melanoma detection and classification: A framework of pixel-based fusion and multilevel features reduction. Microsc Res Tech 2020, http://dx.doi.org/10.1002/jemt.23429.
[137] Xu Y, Lin L, Hu H, Wang D, Zhu W, Wang J, et al. Texture-specific bag of visual words model and spatial cone matching-based method for the retrieval of focal liver lesions using multiphase contrast-enhanced CT images. Int J Comput Assisted Radiol Surg 2018;13(1):151–64.